Hindawi
Journal of Electrical and Computer Engineering
Volume 2023, Article ID 9130209, 11 pages
https://doi.org/10.1155/2023/9130209

Research Article

Energy Sharing of Multiple Virtual Power Plants Based on a Peer Aggregation Model

Sheng Li and Yujie Huang

School of Electric Power Engineering, Nanjing Institute of Technology, Nanjing 211167, China

Correspondence should be addressed to Sheng Li; lisheng_njit@126.com

Received 20 January 2023; Revised 10 October 2023; Accepted 18 December 2023; Published 23 December 2023

Academic Editor: Islam Abdellah

With the increasing number of virtual power plants (VPP) participating in market transactions, the joint operation and energy sharing mode of multiple virtual power plants (multi-VPP) has attracted attention. A peer aggregation model for the multi-VPP energy sharing is proposed based on sharing price. At the VPP autonomous optimization level, each VPP operator formulates an autonomous optimization strategy based on the price incentives and the internal resource parameters and adopts a robust optimization method to improve the strategy's robustness. At the overall level, a sharing level index is introduced to formulate the sharing price mechanism and an overall sharing strategy is proposed. The case simulation results show that compared with the independent operation of each VPP, participating in energy sharing can effectively promote the overall consumption of renewable energy and the overall operating cost is reduced by 18%. The introduction of the sharing level index into the sharing price can effectively improve the rationality of the formulated sharing price, and the net electricity load fluctuation has a greater impact on the system cost than the thermal load fluctuation.

1. Introduction

With the increasing penetration of distributed energy resource (DER), higher requirements are put forward for the flexibility and stability of the large-scale distributed energy power grid-connected system [1–3]. Virtual power plant (VPP) is a power supply coordination management system that participates in the electricity market and power grid operation as a special power plant to realize the aggregation and coordination optimization of all kinds of DERs, including distributed generation, energy storage system, and controllable load and electric vehicle [4]. The proposal of a VPP is one of the important technologies to achieve flexible regulation and coordinated utilization of DERs [5, 6].

In recent years, domestic and foreign scholars have carried out extensive research on the scheduling optimization of single VPP [7–9] and the bidding strategy of VPP participating in market competition [10]. With further opening up of the electricity market, more and more VPPs belonging to different stakeholders begin to participate in electricity market transactions. Therefore, research on VPP is no longer limited to the optimal management of internal resources and has begun to shift to the multi-VPP joint operation and the energy sharing [11].

In reference [12], a multi-VPP noncooperative game model was established, considering the influence of other VPP operation strategies on its own operation strategy, and the model provides ideas for the VPP to participate in the power market competition. The authors of reference [13] built a multi-VPP cooperative game framework based on the block-chain technology, solved the compatibility problem of multi-VPP centralized control, and realized the information interaction and resource sharing among multi-VPPs. Qiu et al. [14] utilized the profit of VPPs to build a noncooperative game model based on the Nash equilibrium, taking into account the economy of power grid and the rationality of bidding of each VPP. In reference [15], a hybrid game-based distribution network, the multi-VPP cooperative strategy, is proposed, and the game model can effectively improve the network's benefits when the interests of lower-level VPPs are taken into account.

However, it is difficult to realize the complex game and analysis of multiagent interests in practical operation. Therefore, in reference [16], an optimal pricing strategy for contract price is built by considering the electricity transactions among multi-VPP. In reference [17], a fuzzy chance constrained source-grid-load coordinated optimal operation method is proposed based on the multiagent system and the multilevel electricity price response mechanism but the level of interaction between the subjects is not considered. In reference [18], a hierarchical coordinated optimization strategy for the multimicrogrid system is proposed but uncertainties are not taken into account when formulating the autonomous strategies. In reference [19], a novel concept of energy shift (ES) was defined, and a market scheme is proposed considering the marginal utility of ES and the transaction between ES and the energy level (EL) so as to integrate VPPs well.

In this paper, a multi-VPP energy sharing model based on a peer aggregation is proposed. First, the multi-VPP energy sharing framework is constructed, the energy sharing center is introduced, and the multi-VPP energy sharing peer aggregation model driven by sharing price is proposed. Second, at the VPP autonomous optimization level, a robust optimization algorithm is used to provide robust decisions against the uncertainty of VPP's internal load and renewable energy, and the autonomous optimization strategy considering the uncertainty of DERs and price incentive signals within each VPP is formulated, so that the supply-demand information is reported to the energy sharing center. On the whole, the overall sharing strategy is proposed. The energy sharing center aggregates and analyzes the sharing information according to the sharing price mechanism and generates the sharing price incentive. The price incentive is released to each VPP to encourage each VPP to participate in the energy sharing, forming an autonomous optimization and interactive iteration of overall sharing. Finally, an example is given to show its effectiveness.

2. Multi-VPP Energy Sharing Framework and the Energy Sharing Model

2.1. Energy Sharing Framework of the VPP Cluster. VPP can gather independent DER together to participate in electricity market transactions. However, the interaction between single VPP and power grid is limited by the market environment, access rules, and physical characteristics, which can easily lead to insufficient wind and photovoltaic consumption and waste of resources. With the continuous opening up of the electricity market, the VPP involved in electricity market transactions has diversified. First of all, each VPP belongs to different stakeholders and is relatively independent. Its operation strategy and internal data have certain privacy. When formulating the joint operation strategy of multi-VPP, the coordination and interaction between each VPP should be fully considered [20]. In addition, in the coordinated scheduling of multi-VPP, only the maximization of the overall benefit is usually considered, and the energy complementarity between VPPs and the compensation optimization of electricity price are ignored. If all the electricity in VPPs is uniformly cleared according to the market competition or the electricity price in the external market, it will inevitably cause damage to some VPP benefits and affect their enthusiasm for participating in the joint operation, thus affecting the overall operation stability and benefit.

This paper constructs a VPP cluster (VPPC) containing multi-VPP and introduces an energy sharing center. The VPPC energy sharing framework is shown in Figure 1. The energy sharing center is a management center established to assist with the energy coordination and sharing in VPPC. Its main role is to match the internal supply-demand information of VPPC and make a reasonable sharing price.

2.2. A Peer Aggregation Model of Energy Sharing. The established peer aggregation model of VPPC energy sharing is shown in Figure 2. According to the price incentive signals and the distributed energy parameters such as wind turbine (WT), photovoltaic (PV), energy storage system (ESS), and combined heat and power (CHP), VPP operators will make internal autonomous optimization strategies to obtain internal supply-demand information and report the information to the energy sharing center.

According to the sharing price strategy, the energy sharing center aggregates and analyzes the overall supply and demand information of VPPC, generates a new price incentive signal, and then publishes the price incentive signal to each VPP. Each VPP will remake the internal autonomy optimization strategy according to the new price incentive signal and report the new supply-demand information to the energy sharing center, so as to form the interaction between the internal autonomous optimization of VPP and the overall coordination and sharing and realize energy sharing.

3. VPP Autonomous Optimization Strategies

Each VPP operator formulates an autonomous optimization strategy with a minimum operating cost based on the internal resource parameters and the sharing price incentive signals.

3.1. Objective Function. The operating cost of VPP mainly considers the internal purchase and sale income of VPP, the fuel cost of the CHP unit, and the maintenance cost of energy storage equipment. Its operating cost function is as follows:

$$C^{\mathrm{vpp}} = \sum_{t=1}^{T}\Big[c_{\mathrm{CHP}}\big(P_t^{\mathrm{GT}} + H_t^{\mathrm{GB}}\big) + \big(I_t^{\mathrm{buy}}P_t^{\mathrm{buy}} - I_t^{\mathrm{sell}}P_t^{\mathrm{sell}}\big) + \lambda_{\mathrm{ESS}}\big(P_t^{\mathrm{cha}} + P_t^{\mathrm{dis}}\big)\Big], \tag{1}$$

where T is the total scheduling period; ${P_t}^{\mathrm{GT}}$ is the power of gas turbine (GT) at time t (kW); H_t^{GT} is the heat power of gas boiler (GB) at time t (kW); c_{CHP} is the fuel cost coefficient (\$/kW); I_t^{buy} is the sharing purchase price and I_t^{sell} is the sharing sell price within VPPC at time t (\$/kW); P_t^{buy} and ${P_t}^{\mathrm{sell}}$ are the electricity demand and supply of VPP,

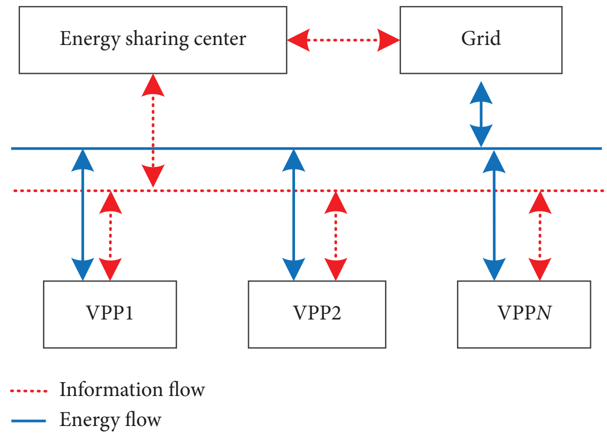

FIGURE 1: VPPC energy sharing framework.

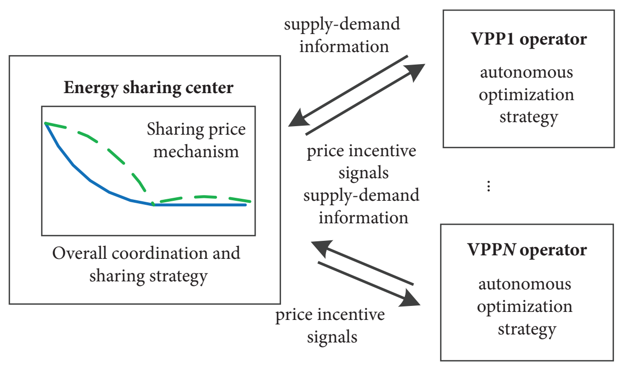

FIGURE 2: Energy sharing peer aggregation model.

respectively, at time t (kW); P_t^{cha} and P_t^{dis} are the charge and discharge power of ESS, respectively, at time t (kW); and λ_{ESS} is the scheduling cost coefficient of ESS (\$/kW).

The objective function in equation (1) is enforced as follows:

$$\begin{cases} 0 \leq P_t^{cha} \leq P_{max}^{cha} U_t^{cha}, \\ 0 \leq P_t^{dis} \leq P_{max}^{dis} U_t^{dis}, \\ U_t^{cha} + U_t^{dis} \leq 1, \\ E_{min} \leq E_t \leq E_{max}, \\ E_t = E_{t-1}(1-\sigma) + \varsigma_{cha} P_t^{cha} - \dfrac{P_t^{dis}}{\varsigma_{dis}}, \end{cases} \tag{2}$$

$$\begin{cases} 0 \leq P_t^{PV} \leq P_{max}^{PV}, \\ 0 \leq P_t^{WT} \leq P_{max}^{WT}, \\ 0 \leq P_t^{GT} \leq P_{max}^{GT}, \\ 0 \leq P_t^{HP} \leq P_{max}^{HP}, \\ 0 \leq H_t^{GB} \leq H_{max}^{GB}, \end{cases} \tag{3}$$

$$\begin{cases} 0 \leq P_t^{buy} \leq P_{max}^{buy}, \\ 0 \leq P_t^{sell} \leq P_{max}^{sell}, \end{cases} \tag{4}$$

where the subscripts "max" and "min" indicate the upper and lower limits, respectively.

The constraints of ESS are given in equation (2). U_t^{cha} and U_t^{dis} are the 0-1 variables of ESS charge and discharge state, respectively, and ς_{cha} and ς_{dis} are the charge and discharge efficiency coefficients of ESS, respectively. E_t is the state of charge (SOC) of ESS at time t, and σ is the self-discharge rate of ESS.

Equation (3) is the running constraints of PV, WT, GT, heat pump (HP), and GB. P_t^{PV}, P_t^{WT}, and P_t^{HP} are the power of PV, WT, and HP, respectively, at time t (kW). The maximum and minimum purchase and sell power of VPP are given in equation (4).

3.2. Uncertain Energy Output Formulation. The renewable energy output and load consumption in VPP are usually obtained by prediction, while the existing prediction methods cannot accurately predict its power. Therefore, it is of practical significance to consider renewable energy and load uncertainty when formulating autonomous optimization strategies. In order to improve the robustness of scheduling results, the worst-case energy balance constraints are constructed by referring to some robust optimization algorithms [21]. The equations are as follows.

3.2.1. Electrical Power Balance

$$\begin{cases} P_t^{\text{buy}} - P_t^{\text{sell}} + P_t^{\text{dis}} - P_t^{\text{cha}} + P_t^{\text{GT}} - P_t^{\text{HP}} = \max\left(P_t^{\text{Load}} - P_t^{\text{WT}} - P_t^{\text{PV}}\right) = P_t^{\text{Load}} - P_t^{\text{WT}} - P_t^{\text{PV}} \\ + \max\left(\eta_{\text{p},t}^{l}\Delta P_{\text{Load},t}^{l} + \eta_{\text{p},t}^{u}\Delta P_{\text{Load},t}^{u} - \eta_{\text{PV},t}^{l}\Delta P_{\text{PV},t}^{l} - \eta_{\text{PV},t}^{u}\Delta P_{\text{PV},t}^{u} - \eta_{\text{WT},t}^{l}\Delta P_{\text{WT},t}^{l} - \eta_{\text{WT},t}^{u}\Delta P_{\text{WT},t}^{u}\right) \\ \text{s.t. } \eta_{\text{p},t}^{l} + \eta_{\text{p},t}^{u} + \eta_{\text{PV},t}^{l} + \eta_{\text{PV},t}^{u} + \eta_{\text{WT},t}^{l} + \eta_{\text{WT},t}^{u} \le \Gamma_{\text{p}}, 0 \le \eta_{\text{p},t}^{l}, \eta_{\text{p},t}^{u}, \eta_{\text{PV},t}^{l}, \eta_{\text{PV},t}^{u}, \eta_{\text{WT},t}^{l}, \eta_{\text{WT},t}^{u} \le 1. \end{cases} \tag{5}$$

In equation (5), P_t^{Load} is the electricity load at time t (kW). $\eta_{p,t}^{l}$, $\eta_{p,t}^{u}$, $\eta_{\text{PV},t}^{l}$, $\eta_{\text{PV},t}^{u}$, $\eta_{\text{WT},t}^{l}$, and $\eta_{\text{WT},t}^{u}$ are the proportional deviations for the random electricity load, PV output, and WT output, respectively. $\Delta P_{\text{load},t}^{l}$, $\Delta P_{\text{load},t}^{u}$, $\Delta H_{\text{load},t}^{l}$, $\Delta H_{\text{load},t}^{u}$, $\Delta P_{\text{PV},t}^{l}$, $\Delta P_{\text{PV},t}^{u}$, $\Delta P_{\text{WT},t}^{l}$, and $\Delta P_{\text{WT},t}^{u}$ represent the allowed maximum deviations with upper and lower bounds. Γ_p is the cardinality budget, which is introduced to adjust the ranges of uncertainty for the net electricity load ($P_t^{\text{Load}} - P_t^{\text{WT}} - P_t^{\text{PV}}$).

3.2.2. Heating Power Balance

$$\begin{cases} H_t^{\text{GT}} + H_t^{\text{GB}} + H_t^{\text{HP}} = H_t^{\text{load}} + \max\left(\eta_{h,t}^{l}\Delta H_{\text{load},t}^{l} + \eta_{h,t}^{u}\Delta H_{\text{load},t}^{u}\right), \\ \text{s.t. } \eta_{\text{h},t}^{l} + \eta_{\text{h},t}^{u} \le \Gamma_{\text{h}}, 0 \le \eta_{\text{h},t}^{l}, \eta_{\text{h},t}^{u} \le 1. \end{cases} \tag{6}$$

In equation (6), H_t^{Load} is the heat load at time t (kW). H_t^{GT}, H_t^{GB}, and H_t^{HP} are the heat power of GT, GB, and HP at time t (kW). $\eta_{h,t}^{l}$ and $\eta_{h,t}^{u}$ are the proportional deviations for the heat load, and $\Delta H_{\text{load},t}^{l}$ and $\Delta H_{\text{load},t}^{u}$ are the allowed maximum deviations. Γ_h is the cardinality budget, which is introduced to adjust the ranges of uncertainty for the heat load.

VPP autonomous optimization is a min-max optimization problem. In order to make the above robust optimization problem easy to solve, we introduce the dual variables to convert the maximization problems into the minimization problems, and it can be expressed as follows:

$$\begin{aligned} &\begin{cases} \min\left(\lambda_{p,t}\Gamma_p + \mu_{P\text{load},t}^{u} + \mu_{P\text{load},t}^{l} + \mu_{\text{PV},t}^{l} + \mu_{\text{PV},t}^{u} + \mu_{\text{WT},t}^{l} + \mu_{\text{WT},t}^{u}\right), \\ \text{s.t. } \lambda_{p,t} + \mu_{P\text{load},t}^{l} \ge \Delta P_{P\text{load},t}^{l}, \lambda_{p,t} + \mu_{P\text{load},t}^{u} \ge \Delta P_{P\text{load},t}^{u}, \\ \lambda_{P,t} + \mu_{\text{PV},t}^{l} \ge \Delta P_{\text{PV},t}^{l}, \lambda_{p,t} + \mu_{\text{PV},t}^{u} \ge \Delta P_{\text{PV},t}^{u}, \\ \lambda_{P,t} + \mu_{\text{WT},t}^{l} \ge \Delta \text{P}_{\text{WT},t}^{l}, \lambda_{P,t} + \mu_{\text{WT},t}^{u} \ge \Delta P_{\text{WT},t}^{u}, \\ \lambda_{P,t}, \mu_{P\text{load},t}^{l}, \mu_{P\text{load},t}^{u}, \mu_{\text{PV},t}^{u}, \mu_{\text{PV},t}^{l}, \mu_{\text{WT},t}^{l}, \mu_{\text{WT},t}^{u} \ge 0, \end{cases} \\ &\begin{cases} \min\left(\lambda_{h,t}\Gamma_h + \mu_{H\text{load},t}^{u} + \mu_{H\text{load},t}^{l}\right), \\ \text{s.t. } \lambda_{h,t} + \mu_{H\text{load},t}^{l} \ge \Delta H_{\text{load},t}^{l}, \\ \lambda_{h,t} + \mu_{H\text{load},t}^{u} \ge \Delta H_{\text{load},t}^{u}, \\ \lambda_{h,t}, \mu_{H\text{load},t}^{l}, \mu_{H\text{load},t}^{u} \ge 0, \end{cases} \end{aligned} \tag{7}$$

where λ_p, λ_h, μ^l_{Pload}, μ^u_{Pload}, $\mu^l_{H\mathrm{load}}$, $\mu^u_{H\mathrm{load}}$, μ^l_{PV}, μ^u_{PV}, μ^l_{WT}, and μ^u_{WT} are the dual variables.

3.3. Overall Coordination and the Sharing Strategy. In order to form the energy sharing within the VPPC, the internal sharing price is used to promote the interaction among VPPs and the internal sharing price is between the prices set by the power grid. That is, the internal sharing sale price of VPPC is higher than that of direct selling electricity to the power grid, and the sharing purchase price is lower than that of direct purchasing electricity from the power grid. At this time, each VPP will actively participate in the internal sharing in order to improve operational benefits. As a result, based on the economic principle that price is inversely proportional to supply-demand ratio [22], the sharing price can be expressed as follows:

$$I_t^{\mathrm{sell}} = \begin{cases} \dfrac{O_t^{\mathrm{buy}} M_t}{\left(\left(O_t^{\mathrm{buy}} - M_t\right)\omega_t + M_t\right)} & 0 \le \omega_t \le 1, \\ I_t^{\mathrm{buy}} \delta_t + O_t^{\mathrm{sell}} \left(1 - \delta_t\right) & \omega_t \ge 1, \end{cases} \tag{8}$$

$$I_t^{\mathrm{buy}} = \begin{cases} I_t^{\mathrm{sell}} \omega_t + O_t^{\mathrm{buy}} \left(1 - \omega_t\right) & 0 \le \omega_t \le 1, \\ \dfrac{O_t^{\mathrm{sell}} M_t}{\left(\left(O_t^{\mathrm{sell}} - M_t\right)\delta_t + M_t\right)} & \omega_t \ge 1, \end{cases} \tag{9}$$

$$\omega_t = \frac{\sum_{K(i\in K)} P_{i,t}^{\mathrm{sell}}}{\sum_{K(i\in K)} P_{i,t}^{\mathrm{buy}}}, \tag{10}$$

where O_t^{buy} and O_t^{sell} are the power grid electricity prices at time t (\$/kW); $P_{i,t}^{\mathrm{sell}}$ and $P_{i,t}^{\mathrm{buy}}$ are the power sold and purchased by i-th VPP at time t (kW); M_t is the middle electricity price at time t (\$/kW), ω_t is the VPPC overall supply-demand ratio at time t; and δ_t is the reciprocal of ω_t.

When $\omega_t = 1$, assuming that the profits of both parties are the same, the internal price should be the average of the power grid purchase and sale price [18]. It can be seen from equations (8) and (9) that if the supply-demand ratio and the grid electricity purchase and sale price are fixed values in different periods, the corresponding sharing price in different periods is the same. This makes the sharing price function unable to reflect changes in the overall sharing level. Therefore, in order to further consider the impact of the overall level of sharing in the formulation of sharing prices, we add the following amendments to the middle price:

$$M_t = O_t^{\mathrm{sell}} + \frac{1}{2}\alpha^{-\left(S_t^{\mathrm{power}}/S_{\max}^{\mathrm{power}}\right)}\left(O_t^{\mathrm{buy}} - O_t^{\mathrm{sell}}\right),$$

$$S_t^{\mathrm{power}} = \begin{cases} \theta^{\mathrm{power,buy}} \sum\limits_{K(i\in K)} \left(P_{i,t}^{\mathrm{sell}} - P_{i,t}^{\mathrm{buy}}\right) & 0 \le \omega_t \le 1, \\ \theta^{\mathrm{power,sell}} \sum\limits_{K(i\in K)} \left(P_{i,t}^{\mathrm{sell}} - P_{i,t}^{\mathrm{buy}}\right) & \omega_t \ge 1, \end{cases} \tag{11}$$

where S_t^{power} is the VPPC sharing level index and $S_{\max}^{\mathrm{power}}$ is the maximum index in a single period; $\theta^{\mathrm{power,buy}}$ and $\theta^{\mathrm{power,sell}}$ are the purchase and sale status indices, respectively, and $\theta^{\mathrm{power,sell}}$ is larger than $\theta^{\mathrm{power,buy}}$; α is a constant; and $1 \le \alpha \le 2$, for example, generally take 1.2.

3.4. Sharing Process. The sharing process is shown in Figure 3. First, we initialize the VPP resource parameters and set the iteration convergence criterion. Second, we set the initial sharing price. Since there is no information aggregation, the initial sharing price is the price of electricity purchased and sold by the grid. Last, each VPP makes an autonomous optimization strategy to obtain their supply-demand information and report it to the energy sharing center. The energy sharing center makes a new sharing price for each VPP according to the aggregation analysis of supply-demand information based on the sharing price strategy to achieve interactive iteration. Once the price change of the two iterations is less than the set value of iteration convergence, the energy sharing and complementary coupling within the VPPC are completed.

The price iteration convergence criterion is as follows:

$$\begin{cases} \Delta I_t^{\mathrm{sell}} = \left| I_t^{\mathrm{sell}}(i+1) - I_t^{\mathrm{sell}}(i) \right|, \\ \Delta I_t^{\mathrm{buy}} = \left| I_t^{\mathrm{buy}}(i+1) - I_t^{\mathrm{buy}}(i) \right|, \\ \max\left\{\Delta I_t^{\mathrm{sell}}, \Delta I_t^{\mathrm{buy}}\right\} \le \varepsilon, \end{cases} \tag{12}$$

where $\Delta I_t^{\mathrm{sell}}$ and $\Delta I_t^{\mathrm{buy}}$ are the changes of two iterations, respectively, ε is the set value of iteration convergence, and i is the current number of iterations.

4. Case Study

A VPPC consisting of VPP1, VPP2, and VPP3 is used for the numerical analysis, and the three VPPs have similar geographical locations and obvious differences in power generation and load characteristics. VPP1's load is an industrial load. VPP2's load is a commercial load. VPP3's load is a resident load. The DERs of VPP1 and VPP3 are both wind turbines, and the DER of VPP2 is PV power generation. Figure 4 shows the change curves of the electricity load, heat load, and WT/PV output of VPP1~VPP3 (the data refer to reference [23]). It can be seen from Figure 4 that VPP1 maintains a higher electricity load level from 6:00 to 20:00, but VPP3 has an electricity peak only in the evening. VPP2 has two electricity peaks at the periods 5:00–8:00 and 17:00–20:00.

The parameters of time-of-use electricity price in 24 hours are the same as in reference [15], and among them, the electricity purchase price refers to reference [23].

From 23:00 today to 7:00 the next day, the purchase price is 0.4 \$/kWh and the sale price is 0.2 \$/kWh.

From 7:00 to 11:00 and from 14:00 to 18:00, the purchase price is 0.75 \$/kWh and the sale price is 0.4 \$/kWh.

From 11:00 to 14:00 and from 18:00 to 23:00, the purchase price is 1.2 \$/kWh and the sale price is 0.6 \$/kWh.

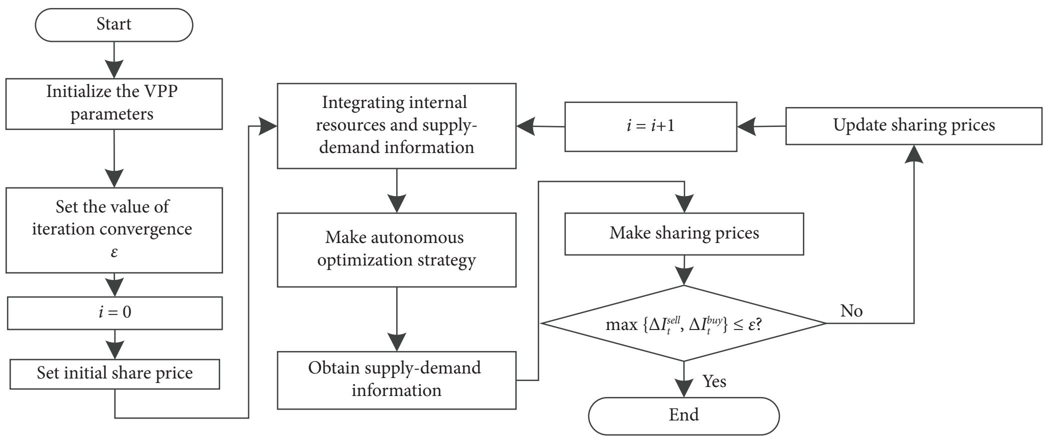

Figure 3: Sharing process.

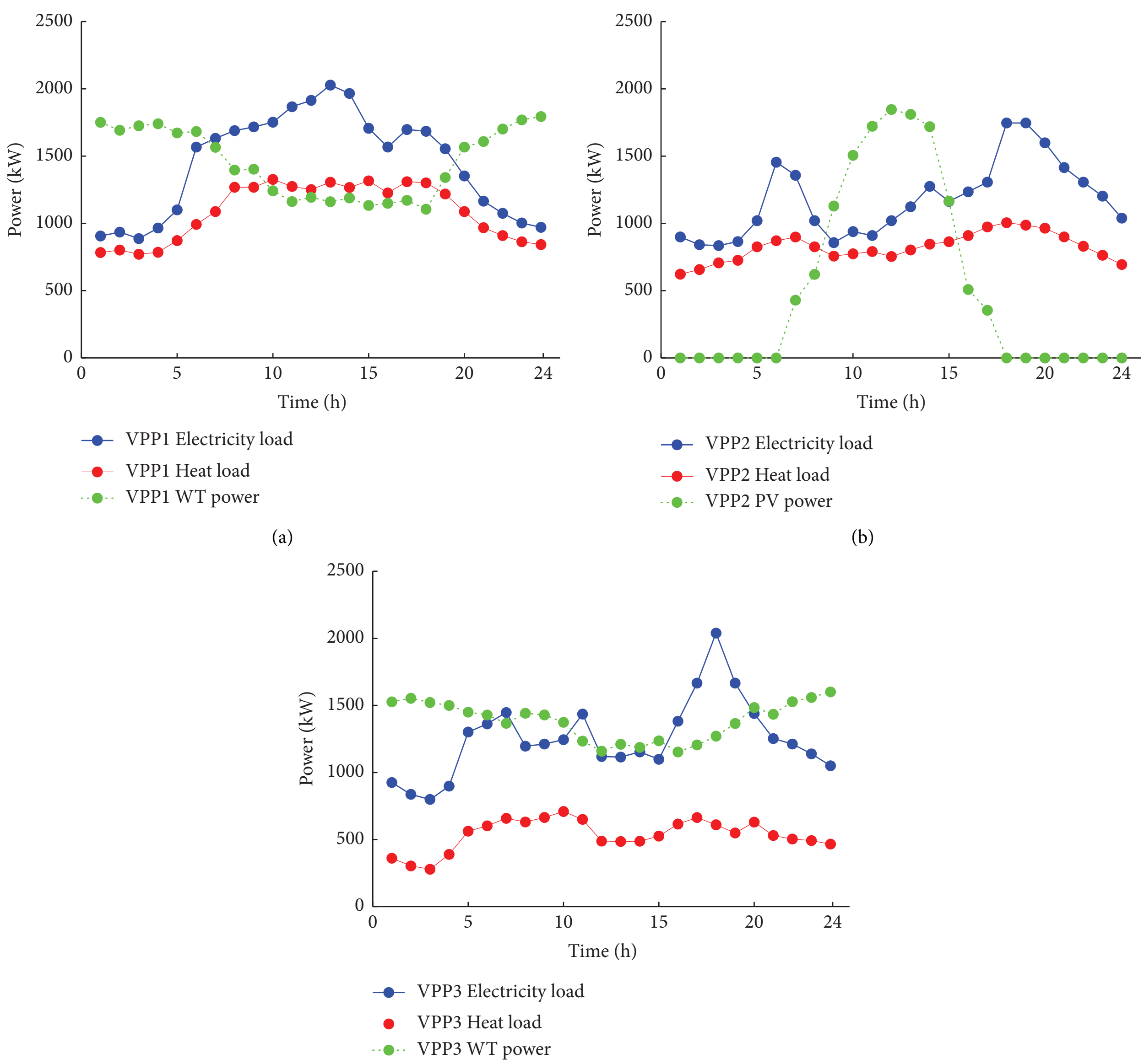

Figure 4: Load and power output curves of VPPs. (a) VPP1. (b) VPP2. (c) VPP3.

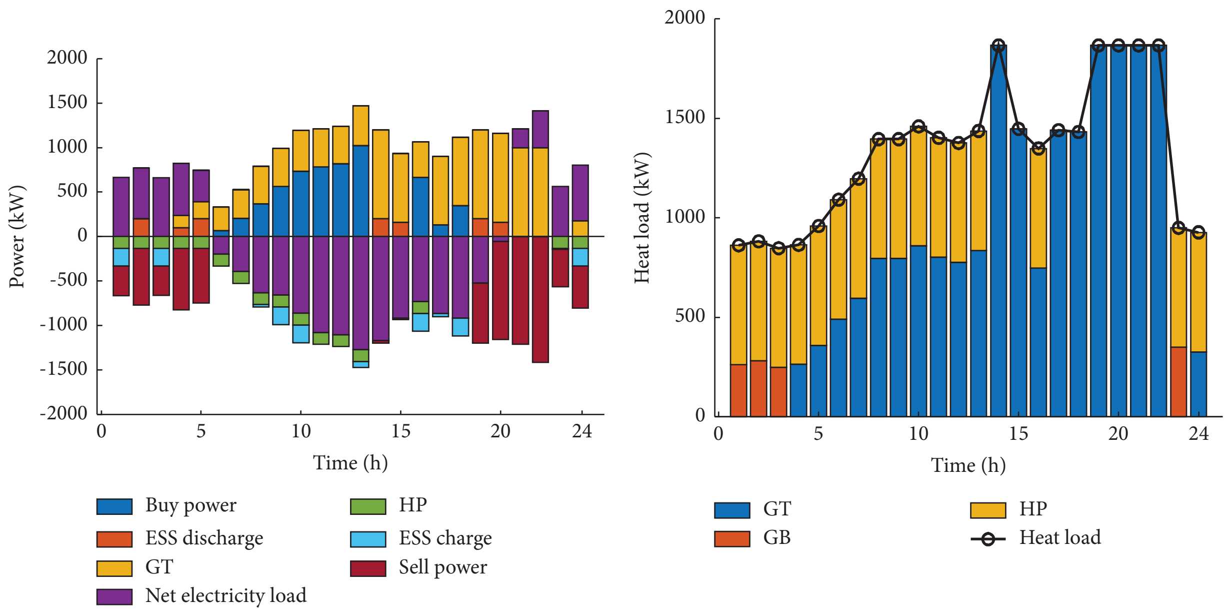

(a) (b)

Figure 5: Dispatch results by VPP1. (a) Electricity power balance. (b) Heat power balance.

This example is only used for the simulation verification in this paper and does not combine with the actual system parameters.

4.1. Result Analysis. The dispatch results of each VPP participating in energy sharing are shown in Figures 5–7. It can be seen from Figures 5–7 that each VPP achieves the electricity power balance and the heat power balance, and the optimization results are effective.

It can be seen from Figures 4(a) and 5 that due to the industrial load within VPP1, there is a large demand to meet and has been in the state of purchasing electricity from other VPPs or the power grid in the period 6:00–18:00. In other periods, VPP1 has a smaller electricity load and a larger wind power output. VPP1 is oversupplied; due to the CHP works in the "ordering power by heat" mode, it can sell electricity to other VPPs or the power grid. Through energy sharing, VPP1 can consume the surplus wind power resources within it and can also sell electricity to other VPPs in the VPPC under the guidance of the sharing price.

It can be seen from Figures 4(b) and 6 that at two electricity peaks of VPP2, the PV output is at a low level, but VPP1 and VPP3 have more electricity surpluses, so VPP2 can purchase electricity from other VPPs to meet load demands by energy sharing. In the period 9:00–15:00, VPP2's PV output is at a high level and the load is in the low stage. At this time, VPP2 can sell electricity to the outside through the energy sharing center to reduce the phenomenon of light abandonment.

It can be seen from Figures 4(c) and 7 that VPP3's WT output is relatively stable throughout the day, and the internal resident load only in the evening has a higher load demand, so VPP3 has the residual energy supply to other VPPs.

Combined with the power balance analysis of the three abovementioned VPPs, it can be seen that although the power generation and load characteristics of each VPP are significantly different, the buying and selling behaviors are generally consistent. The energy sharing reduces each VPP's operating costs and operational pressure. The internal ESS, GT, and other resources can also cooperate well with the operation of each VPP.

4.2. Sharing Strategy Analysis. The mechanism of changing sharing prices with the supply-demand ratio is depicted in Figure 8. In Figure 8, the sharing price 1 is the period $S_t^{\text{power}} < 0$ and the sharing price 2 is the period $S_t^{\text{power}} > 0$. It can be seen from Figure 8 that in the same period of supply-demand ratio and electricity price, the sharing price with large S_t^{power} is low and the sharing price with small S_t^{power} is high. Therefore, internal energy sharing is preferred when the overall sharing level is low and VPPs reduce interaction with the power grid to ensure economic benefit.

Figure 9 shows the electricity price mechanism diagram at each moment. It can be seen that the actual price satisfies the fact that the sharing price is always between the grid purchase price and sale price, and the sharing sale price is lower than the sharing purchase price, which verifies the rationality of the established sharing price.

It can be seen from Figure 9 that the supply is less than the demand in the periods 5:00–7:00, 14:00–15:00, and 19:00–20:00 and the transaction price is higher; in the period 8:00–13:00, supply exceeds demand and the transaction price is low. On the other hand, combining with Figure 8, we can see that the overall sharing level is reflected by the intermediate price. The sharing price is higher than the middle price, VPPC presents a purchasing state, and the overall level of sharing is low. On the contrary, the overall level of sharing is high.

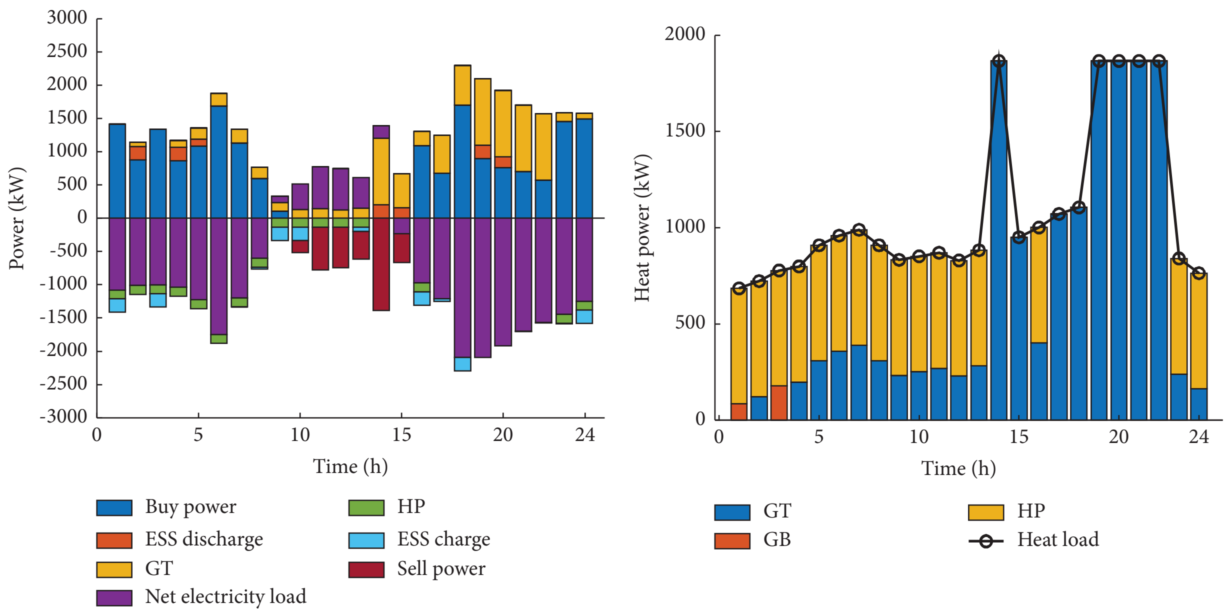

(a) (b)

Figure 6: Dispatch results by VPP2. (a) Electricity power balance. (b) Heat power balance.

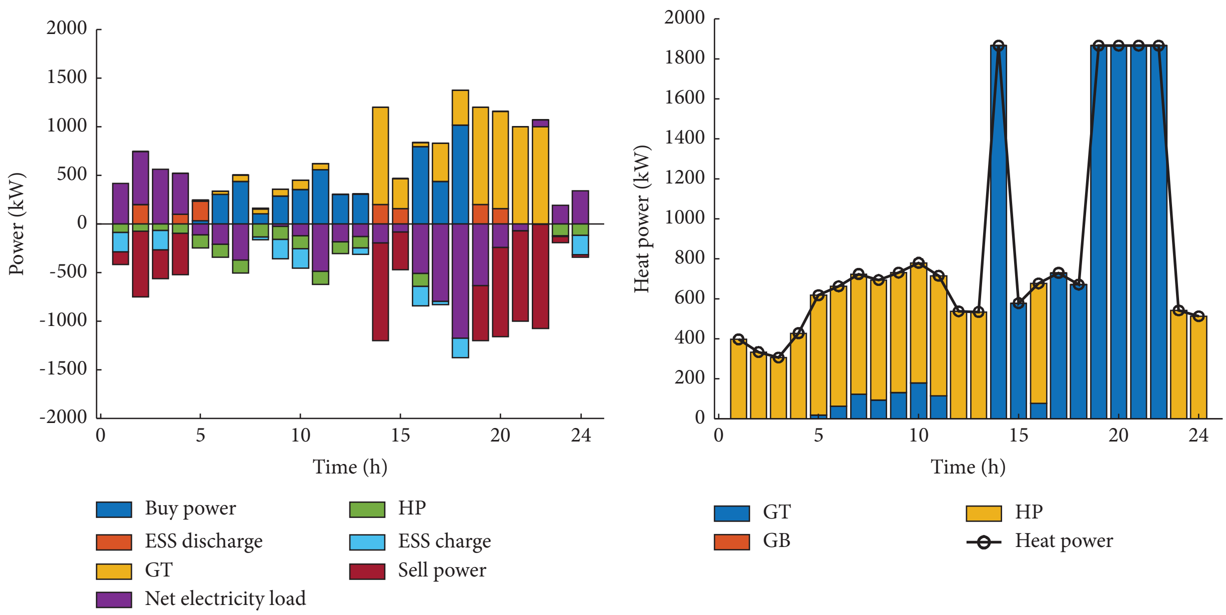

(a) (b)

Figure 7: Dispatch results by VPP3. (a) Electricity power balance. (b) Heat power balance.

To further embody the superiority of energy sharing, we compare the total operating cost of each VPP running separately and participating in coordinated operation. The total cost of each VPP running independently is 32124.5 $ and the total cost of participating in energy sharing is 26314.0 $. The cost is reduced by 18%.

Using the proposed pricing scheme in references [18, 22], the operation costs are 26411.0 $ and 26238.7 $, which are basically similar to this paper. Therefore, the internal energy interactions are further compared, as shown in Table 1. From Table 1, it can be seen that the internal energy interactions in this paper are significantly enhanced, which is conducive to promote the consumption of renewable energy and reduce the interaction with the grid.

4.3. Robust Parameter Analysis. In order to verify the influence of budget cardinality selection on the conservative degree of autonomous optimization strategy formulation, we select VPP1 to interact with the power grid alone as an

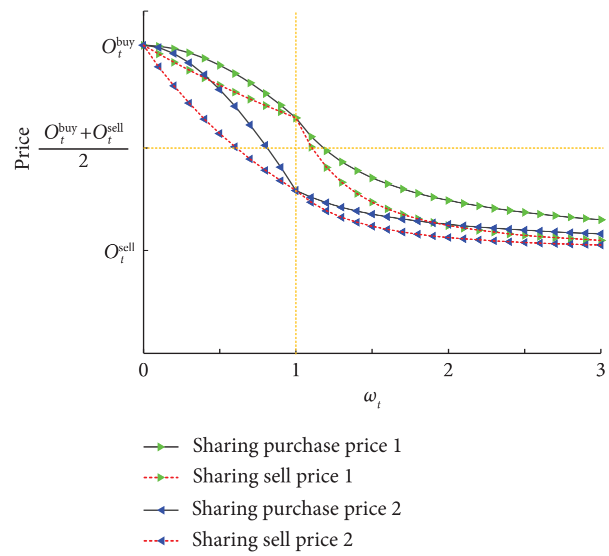

FIGURE 8: Sharing price mechanism.

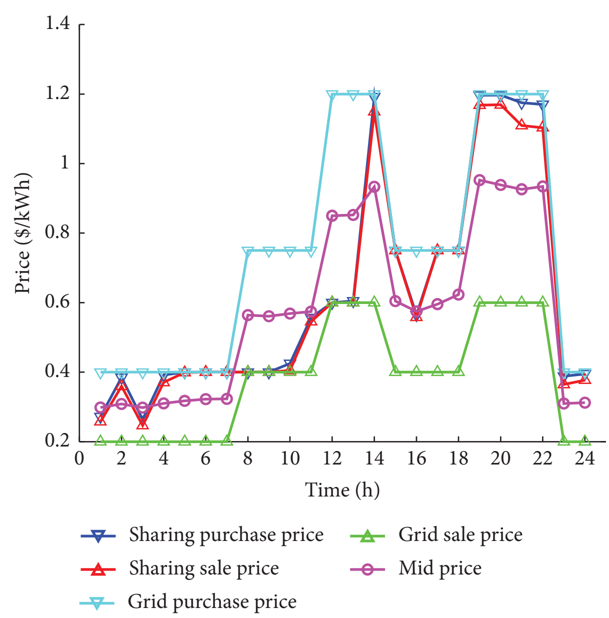

FIGURE 9: Electricity price diagram at each moment.

TABLE 1: Comparison of energy interaction under different schemes.

Schemes	Buy power (kW)	Sell power (kW)	Internal interaction (kW)
Pricing scheme of reference [22]	29875.6	13562.0	5450.1
Pricing scheme of reference [18]	27593.5	17702.3	8915.4
Sharing price	29187.1	17934.3	9259.5

TABLE 2: Changes in the operating cost under case 1.

Γ_p	Cost ($)	Increased %
0.0	7059.7	0.0
0.2	7784.4	10.27
0.5	8964.3	26.98
0.8	10195.9	44.42
1.0	11080.3	56.95

Table 3: Changes in the operating cost under case 2.

Γ_h	Cost ($)	Increased %
0.0	10255.0	0.00
0.2	10418.6	1.59
0.5	10665.0	3.99
0.8	10913.6	6.42
1.0	11080.3	8.05

example to observe the change of operating cost when the budget cardinality (Γ_p or Γ_h) changes in two scenarios.

(1) Case 1: $\Gamma_h = 1$, Γ_p increased from 0 to 1.

(2) Case 2: $\Gamma_p = 1$, Γ_h increased from 0 to 1.

Tables 2 and 3 show the changes in the operating cost in the abovementioned two scenarios.

From Tables 2 and 3, it can be seen that net electricity load fluctuation has a much greater impact on operating costs than the heat load fluctuation. When the increase of Γ_p starts from 0 to 1, the overall operation cost of VPP1 increases by 56.95%, and the cost of VPP1 increases by 8.05% when the increase of Γ_h starts from 0 to 1. It is verified that the uncertain budget parameters have a certain impact on the system's economy. Therefore, selecting the appropriate robust parameters according to the historical data and operation requirements can improve the economy of the formulated operation strategy.

5. Conclusions

This paper investigates an energy sharing framework for multi-VPP with different characteristics in adjacent areas and proposes an energy sharing peer aggregation model for multi-VPP driven by sharing price. The following conclusions can be obtained:

(1) The multi-VPP energy sharing peer aggregation model publishes the sharing price incentives through the energy sharing center and guides VPPs to achieve autonomous operation according to the sharing price incentives. It can give full play to the autonomous optimization ability of each VPP, mobilize the enthusiasm of VPPs to participate in sharing, and achieve multi-VPP energy sharing in the region.

(2) The established sharing price mechanism according to the supply and demand relationship of electric energy improves the income of each VPP participating in internal transactions, and on this basis, the sharing level index is introduced to guide VPPs to actively participate in energy sharing. Through a case analysis, this sharing price is reasonable and can effectively improve the operation efficiency of each VPP.

(3) The robustness of the VPP autonomous strategy is improved by the robust optimization algorithm with the budget cardinality. VPP operators can select appropriate robust parameters with historical data and operation requirements to improve the economy and robustness of the strategy.

Data Availability

The data used to support the findings of this study are included within the article.

Conflicts of Interest

The authors declare that they have no conflicts of interest.

Acknowledgments

This work was partially supported by the Scientific Research Foundation of the Nanjing Institute of Technology (Grant no. ZKJ202102).

References

[1] J. Sun, Y. Wang, X. Guo, Y. Zhou, Y. Wang, and W. Xue, "Optimal operation of virtual power plant considering environmental externality and output uncertainty of wind and photovoltaic power," *Automation of Electric Power Systems*, vol. 46, no. 8, pp. 50–59, 2022.

[2] S. Li, Y. Lu, and Y. Ge, "Static voltage stability zoning analysis based on a sensitivity index reflecting the influence degree of photovoltaic power output on voltage stability," *Energies*, vol. 16, no. 6, p. 2808, 2023.

[3] S. Li, Z. Zhou, Q. Shan, and J. An, "Analysis of transient voltage stability in a low voltage distribution network using SST for the integration of distributed generations," *Journal of Electrical and Computer Engineering*, vol. 2018, Article ID 3498491, 9 pages, 2018.

[4] Z. Wei, S. Yu, G. Sun, Y. Sun, Y. Yuan, and D. Wang, "Concept and Development of virtual power plant," *Automation of Electric Power Systems*, vol. 37, no. 13, pp. 1–9, 2013.

[5] J. Li and Q. Ai, "Operation mode of virtual power plant considering peak regulation auxiliary service," *Electric Power Automation Equipment*, vol. 41, no. 6, pp. 1–7, 2021.

[6] L. Liu, N. Luo, T. Wu, and W. Zheng, "Optimal scheduling of virtual power plant considering demand side integer second-order cone programming," *Acta Energiae Solaris Sinica*, vol. 42, no. 8, pp. 96–104, 2021.

[7] H. Zhao, B. Wang, X. Wang et al., "Active dynamic aggregation model for distributed integrated energy system as virtual power plant," *Journal of Modern Power Systems and Clean Energy*, vol. 8, no. 5, pp. 831–840, 2020.

[8] J. Lee and D. Won, "Optimal Operation strategy of virtual power plant considering real-time dispatch uncertainty of distributed energy resource aggregation," *IEEE Access*, vol. 9, pp. 56965–56983, 2021.

[9] F. Fang, S. Yu, and X. Xin, "Data-driven-based stochastic robust optimization for a virtual power plant with multiple uncertainties," *IEEE Transactions on Power Systems*, vol. 37, no. 1, pp. 456–466, 2022.

[10] W. Hongliang, L. Benjie, P. Daoxin, and W. Ling, "Virtual power plant participates in the two-level decision-making optimization of internal purchase and sale of electricity and external multi-market," *IEEE Access*, vol. 9, pp. 133625–133640, 2021.

[11] Y. Wang, X. Ai, Z. Tan, L. Yan, and S. Liu, "Interactive dispatch modes and bidding strategy of multiple virtual power plants based on demand response and game theory," *IEEE Transactions on Smart Grid*, vol. 7, no. 1, pp. 510–519, 2016.

[12] B. Zhou, L. Lü, H. Gao, J. Liu, Q. Chen, and X. Tan, "Robust day-ahead trading strategy for multiple virtual power plants," *Power System Technology*, vol. 42, no. 8, pp. 2694–2703, 2018.
[13] B. Zhou, Y. Zhang, T. Zang, Q. Cao, H. Zhang, and H. Peng, "Blockchain-based stackelberg game optimal operation of multiple virtual power plants," *Automation of Electric Power Systems*, vol. 46, no. 1, pp. 155–163, 2022.
[14] G. Qiu, X. Yu, Y. Jin, C. He, Y. Lou, and A. Yang, "Economic dispatching of regional power grid based on multi-virtual power plant game," *Proceedings of the CSU-EPSA*, vol. 33, no. 6, pp. 75–83, 2021.
[15] Y. Huang, "Hybrid game-based distribution network and multi-virtual power plant co-optimization," *Journal of Energy Research and Reviews*, vol. 14, no. 2, pp. 24–32, 2023.
[16] Y. Chen, Z. Wei, Z. Xu, W. Huang, G. Sun, and Y. Zhou, "Optimal scheduling strategy of multiple virtual power plants under electricity market reform," *Automation of Electric Power Systems*, vol. 43, no. 7, pp. 42–49, 2019.
[17] X. Xu, Y. Song, L. Yao, R. Suo, and Z. Yan, "Source-grid-load coordination method for active distribution network based on multi-level electricity price response mechanism," *Automation of Electric Power Systems*, vol. 42, no. 5, pp. 9–17, 2018.
[18] H. He, X. Lei, T. Huang, and J. He, "Coordinated and autonomous optimal operation strategy of multi-microgrid system under the guidance of price," *Power System Protection and Control*, vol. 47, no. 16, pp. 17–26, 2019.
[19] S. Fan, J. Xiao, Z. Li, and G. He, "Characterization and trading of energy level and energy shift considering virtual power plant," *Journal of Modern Power Systems and Clean Energy*, vol. 10, no. 6, pp. 1784–1789, 2022.
[20] F. Liu, Y. Xu, X. Yang, L. Li, G. Fu, and Z. Chai, "Multi-time scale coordinated operation strategy of virtual power plant clusters considering power interactive sharing," *Power System Technology*, vol. 46, no. 2, pp. 642–656, 2022.
[21] Z. Cheng, D. Jia, Z. Li, J. Si, and S. Xu, "Multi-time scale dynamic robust optimal scheduling of CCHP microgrid based on rolling optimization," *International Journal of Electrical Power & Energy Systems*, vol. 139, Article ID 107957, 2022.
[22] N. Liu, X. Yu, C. Wang, C. Li, L. Ma, and J. Lei, "Energy-sharing model with price-based demand response for microgrids of peer-to-peer prosumers," *IEEE Transactions on Power Systems*, vol. 32, no. 5, pp. 3569–3583, 2017.
[23] M. Cui, M. Xuan, Z. Lu, and L. He, "Operation optimization strategy of multi integrated energy service companies based on cooperative game theory," *Proceedings of the CSEE*, vol. 42, no. 10, pp. 3548–3563, 2022.